

Role of transition zones in marine ice sheet dynamics

Frank Pattyn,¹ Ann Huyghe,² Sang De Brabander,² and Bert De Smedt²

Received 11 August 2005; revised 3 January 2006; accepted 23 January 2006; published 26 April 2006.

[1] It has been suggested that rapid thinning of the West Antarctic ice sheet is due to increased melting under ice shelves caused by a gradual ocean warming (Shepherd et al., 2004). Payne et al. (2004) showed that such melting could lead to an acceleration of grounded ice flow. In this paper, we analyze the response of a marine ice sheet to different perturbations near the grounding line using a numerical ice sheet model that takes into account longitudinal stress coupling and grounding line migration at subgrid precision, based on a novel technique. Results show that stress transmission or longitudinal coupling across the grounding line plays a decisive role. The grounding line migration is a function of the length scale over which the basal conditions change from frozen to the bed to floating, the “transition zone.” We demonstrate that thinning of the ice shelf due to bottom melting has a negligible effect on the grounded ice mass. Only perturbations at the grounding line or reduction in buttressing of the ice shelf substantially thins the grounded ice sheet. Inclusion of lateral drag does not alter these results qualitatively. Marine ice sheets with large transition zones, such as ice streams, seem highly sensitive to such perturbations compared to ice sheets with small transition zones, such as an abrupt ice sheet/ice shelf junction.

Citation: Pattyn, F., A. Huyghe, S. De Brabander, and B. De Smedt (2006), Role of transition zones in marine ice sheet dynamics, *J. Geophys. Res.*, *111*, F02004, doi:10.1029/2005JF000394.

1. Introduction

[2] Recent changes in ice volume of the Antarctic ice sheet and the West Antarctic Ice Sheet (WAIS) in particular raise new questions on the mechanisms responsible for enhanced ice loss. On the basis of satellite altimetry, *Wingham et al.* [1998] reported a thinning of the WAIS of $53 \pm 9 \text{ mm yr}^{-1}$, largely located in the Pine Island (PIG) and Thwaites Glacier basins. The measurements of *Rignot* [1998], showing a $1.2 \pm 0.3 \text{ km yr}^{-1}$ retreat of the grounding line of PIG between 1992 and 1996, suggest an ice dynamic explanation for the observed thinning. According to *Shepherd et al.* [2004], increased melting under ice shelves caused by a gradual ocean warming would be responsible for this. Ice shelf thinning would cause an acceleration of grounded ice flow, inevitably leading to an increased ice discharge in the ocean [*Payne et al.*, 2004].

[3] Marine ice sheets rest on a bed that lies well below sea level and the drainage of the ice sheet (necessary to balance the ice accumulation) takes place through surrounding ice shelves. Marine ice sheet stability is believed to be controlled by dynamics of the grounding line, i.e., the junction between the grounded ice sheet and the floating ice shelf. The WAIS has therefore received particular

attention because it has been the most dynamic part of the Antarctic ice sheet in the recent geological past, and because most of it is grounded below sea level, a situation that according to early models, could lead to flow instabilities and rapid ice discharge into the ocean when the surrounding ice shelves would weaken [*Thomas*, 1973; *Thomas and Bentley*, 1978]. Such instability is governed by the physical interaction between ice streams and shelves, more precisely the feedback between grounding lines and ice flux. The potential of the WAIS to collapse in response to future climate change is still a subject of debate and controversy. If the entire WAIS would collapse, global sea level would rise by 5 to 6 m [*Bentley*, 1998].

[4] Grounding line migration is a key element in assessing the stability of marine ice sheets, and the WAIS in particular [*Vieljeux and Payne*, 2005]. We believe that stress transfer or longitudinal stress coupling across the grounding line plays a decisive role herein and is determined by the length of the transition zone between ice sheet and ice shelf. Such transition can be small, i.e., an abrupt change from ice sheet to ice shelf, or large when an ice stream makes the linkage between both systems. As pointed out by *Van der Veen* [1999], the early WAIS model mentioned above [*Thomas*, 1973; *Thomas and Bentley*, 1978] had some severe shortcomings, such as the inconsistency in incorporating ice shelf dynamics, neglecting advection of inland ice as a response to changes at the grounding line, and keeping a constant length of the transition zone with time. A more rigorous approach is presented by *Van der Veen* [1985], who concludes that a collapse of the ice sheet, caused by increased melting of ice shelves, is not very likely. The *Van der Veen* model included longitudinal stress coupling

¹Laboratoire de Glaciologie, Département des Sciences de la Terre et de l'Environnement, Université Libre de Bruxelles, Brussels, Belgium.

²Department of Geography, Vrije Universiteit Brussel, Brussels, Belgium.

by determining the vertically averaged longitudinal stress deviator, but was only valid for relatively small transition zones, parameterized in such a way that the influence of the stress deviator decreased rapidly toward the interior. *Hindmarsh* [1993] confirms that such a transition zone is of limited extent and that it is unlikely that stress transmission takes place. This idea is based on results by *Whillans and Van der Veen* [1993], which show that gradients in longitudinal stress offer little resistance to the ice flow. The transition from basal drag control to ice shelf flow is achieved through reduced drag at the glacier base and increased resistance associated with lateral drag. Model calculations by *Herterich* [1987] and *Lestringant* [1994] underscore the idea of negligible impact of (freely floating) ice shelves. The implication of this is that ice shelves do not need to be included in prognostic marine ice sheet models.

[5] How grounding lines should react to given environmental conditions was investigated during the European Ice Sheet Model Intercomparison (EISMINT) exercise [*Huybrechts et al.*, 1998] and revealed that all participating numerical models gave different results. The dependency on horizontal grid size, hence grid jumping of the grounding line, might be responsible for this [*Vieli and Payne*, 2005]. The problem can be overcome by using a moving grid model, propelled by an expression of the grounding line migration rate [*Hindmarsh*, 1993; *Hindmarsh and Le Meur*, 2001]. However, such an approach automatically reduces the influence of effects at the seaward side of the grounding line, as grounding line migration becomes independent of the presence of an ice shelf.

[6] The need for elaborate models that treat both the mechanical coupling between ice shelf and ice sheet and simulate the migration of the grounding line in an appropriate way becomes clear after the recent study by *Payne et al.* [2004], who showed that effects of perturbations at the grounding line (a reduction in friction) have a major influence on PIG's dynamics, due to rapid upstream thinning propagation. Although their model experiments were prognostic, the grounding line was not allowed to move dynamically. *Dupont and Alley* [2005], using a simplified but dynamic model, show that reduction or loss of a restraining ice shelf causes speedup of inland ice flow. Field evidence for loss of buttressing comes from the Antarctic Peninsula, where interferometric synthetic aperture radar data collected by ERS-1/2 and Radarsat-1 satellites as well as Landsat 7 images acquired between January 2000 and February 2003 show a twofold to sixfold increase in centerline speed of glaciers following the collapse of Larsen B ice shelf in 2002 [*Rignot et al.*, 2004; *Scambos et al.*, 2004]. All these studies thus imply a tight coupling between the ice sheet interior and surrounding ocean.

[7] In this paper, we try to shed a light on both mechanisms of stress transmission and grounding line migration in a marine ice sheet for different perturbations in both the ice shelf and at the grounding line, and for different types/sizes of transition zones. Longitudinal stress coupling across the grounding line is taken into account, based on the higher-order model of *Pattyn* [2002]. A novel approach is the determination of the grounding line with subgrid precision and its direct coupling to the basal boundary condition in terms of a basal friction parameter, also at subgrid level. The

disability of fixed grid models to cope with grounding line migration is thereby overcome.

2. Model Description

[8] The numerical ice sheet model is a two-dimensional finite difference model on a fixed grid in space and time (flow line model) that includes vertical shear and longitudinal stress gradients [*Pattyn*, 2002]. The horizontal stress balance reads

$$4 \frac{\partial}{\partial x} \left(\eta \frac{\partial u}{\partial x} \right) + \frac{\partial}{\partial z} \left(\eta \frac{\partial u}{\partial z} \right) = \rho_i g \frac{\partial z_s}{\partial x}, \quad (1)$$

where $\eta = 1/2A^{-1/n}\dot{\epsilon}^{(1-n)/n}$ is the ice viscosity, u is the horizontal velocity, $\dot{\epsilon}$ is the effective strain rate, z_s is the ice sheet surface elevation, A is the flow parameter taken as $1.4 \times 10^{-17} \text{ Pa}^{-3} \text{ yr}^{-1}$ [*Vieli and Payne*, 2005], ρ_i is the ice density (910 kg m^{-3}) and g is the gravitational acceleration (9.81 m s^{-2}). Equation (1) is derived from conservation of linear momentum, thereby making two major assumptions, i.e., hydrostatic approximation in the vertical or $\partial\sigma_{zz}/\partial z \approx \rho g$, and $\partial w/\partial x \ll \partial u/\partial z$ [*Pattyn*, 2002, 2003]. At the upstream boundary a symmetric ice divide is considered ($\partial z_s/\partial x = 0$) and at the downstream boundary (shelf-ocean boundary) the longitudinal stress gradient is balanced by the hydrostatic pressure of the ocean water [*Paterson*, 1994]:

$$\frac{\partial u}{\partial x} \Big|_e = A\sigma_e^n = A \left[\frac{1}{4} \rho_i g h \left(1 - \frac{\rho_i}{\rho_w} \right) \right]^n, \quad (2)$$

where ρ_w is the density of seawater (1028 kg m^{-3}), h is the ice thickness, and σ_e is the tensile deviatoric stress at the ice shelf front. The ice/air interface is considered a stress free surface. At the base, a linear sliding law is introduced of the form $\tau_b = u_b \beta^2$, where β^2 is a friction parameter [*MacAyeal*, 1993], relating basal velocity to the basal drag. As such, the lower boundary condition reads

$$4\eta \frac{\partial u_b}{\partial x} \frac{\partial z_b}{\partial x} - 2\eta \frac{\partial u_b}{\partial z} - u_b \beta^2 = 0 \quad (3)$$

where z_b is the subglacial elevation (bedrock elevation in case the ice sheet is grounded). More details on the determination of β^2 are given in section 2.2. The time-dependent response of the ice sheet is then given by the continuity equation

$$\frac{\partial h}{\partial t} = \dot{a} - \dot{m} - \frac{\partial q}{\partial x}, \quad (4)$$

where t is time, \dot{a} the surface mass balance, \dot{m} is basal melting and $q = \bar{u}h$ is the horizontal flux of ice. Details on the numerical solution of the continuity equation are given in Appendix A.

2.1. Determining the Grounding Line Position

[9] The position of the grounding line can be determined in a number of ways. Most ice sheet models developed on a regular (fixed) grid determine the position of the grounding line as the last grid point of the grounded ice sheet, the next

downstream grid point being an ice shelf node [e.g., *Huybrechts*, 1992]. The flotation condition is used to decide where the ice is grounded or is part of the ice shelf, which is given by

$$\rho_i h = \rho_w (z_{sl} - b), \quad (5)$$

where z_{sl} is the height of the sea level and b the bedrock elevation. Another way of determining the position of the grounding line is based on an expression for the grounding line migration rate to compute the grounding line motion. Following *Hindmarsh* [1996] and *Vieli and Payne* [2005], from a total differentiation of the flotation condition (5) and through substitution of (4), the grounding line migration rate is given by

$$\frac{dx_g}{dt} = \frac{\rho_w \frac{\partial(z_{sl} - b)}{\partial t} + \dot{a} - \dot{m} - \frac{\partial q}{\partial x}}{\frac{\partial h}{\partial x} - \frac{\rho_w}{\rho_i} \frac{\partial(z_{sl} - b)}{\partial x}}, \quad (6)$$

where x_g is the position of the grounding line. All variables are evaluated at the grounding line. Using (6) there is no need for an ice shelf, as the position of the grounding line is solely determined from geometry at the grounding line, local ice flux and accumulation rate. To accurately determine the motion of the grounding line a normalized horizontal coordinate must be introduced, leading to a moving grid model. Although such type of model is convenient along a flow line, its application is much more tedious in the plane.

[10] In this paper we use a trade-off between the fixed grid model and the precise determination of the grounding line using (6), i.e., the position of the grounding line is determined with subgrid precision based on the flotation criterion (5). Consider the function

$$f = \frac{(z_{sl} - b)\rho_w}{\rho_i h}. \quad (7)$$

It follows that $f = 1$ at the grounding line, $f < 1$ in the grounded ice sheet, and $f > 1$ in the ice shelf. The exact position of the grounding line x_g (km) is then defined by linear interpolation of (7) between the last grounded j and the first floating grid point $j + 1$:

$$x_g = \frac{1 - f_j + \nabla f x_j}{\nabla f}, \quad (8)$$

where $\nabla f = (f_{j+1} - f_j)/\Delta x$. This scheme has the advantage that it can be easily translated to the plane. Such procedure still requires an interpolation between variables near the grounding line and will thus remain affected by the grid size. Nevertheless, the moving grid model also requires a remapping, as a grounding line advance requires stretching of the coordinate system and calculating ice thickness gradients at the exact grounding line position. *Vieli and Payne* [2005] found such interpolation unaffected by grid size changes.

2.2. Stress Transfer Across the Grounding Line

[11] Most numerical models that include grounding line dynamics do this in a simplified way. The velocity field

within the grounded ice sheet is determined using the shallow ice approximation [*Hutter*, 1983], which is similar to neglecting the horizontal velocity gradients $\partial u/\partial x$ in (1). The ice shelf is then modeled by neglecting the vertical velocity gradients $\partial u/\partial z$ in (1) and by integrating this equation over the vertical. This results in an equation similar to (2). The ice sheet/ice shelf distinction is made using (5), which means that the transition zone is considered to be small, i.e., less than the horizontal grid size. Some models do take longitudinal stress gradients at the grounding line in a vertically averaged way, but still consider the transition zone smaller than a grid size [*Van der Veen*, 1985; *Huybrechts*, 1992]. Moving grid models [*Hindmarsh and Le Meur*, 2001] are also based on the shallow ice approximation. Some of the experiments presented by *Vieli and Payne* [2005] consider an ice shelf glued to the ice sheet, or an ice shelf glued to an ice stream model (which is an ice shelf model considering basal traction [e.g., *MacAyeal*, 1993]). In the first case, stress transmission across the grounding line is not possible; in the second case (ice stream/ice shelf junction) longitudinal stress transmission exists.

[12] Determining the length of the transition zone is crucial for understanding grounding line migration. As shown by *Mayer and Huybrechts* [1999], transition zones at the ice sheet/ice shelf junction along the East Antarctic coast are narrow. Although this type of transition is common along the perimeter of the Antarctic ice sheet, most of the ice discharge across the grounding line happens through larger outlet glaciers and ice streams. These features have the tendency of widening the transition zone, as they are characterized by a significant amount of basal sliding, hence a low basal friction. In that case the shallow ice approximation is not viable anymore, and other stress gradients, such as transverse and longitudinal stress gradients, must develop in order to fulfill the balance of forces. The onset of these fast flowing features is then another kind of transition zone, i.e., the zone between the ice sheet that is well coupled (and mostly frozen) to the bed and the well-lubricated ice stream (Figure 1). *Hulbe and MacAyeal* [1999] combine an ice sheet, ice stream, and ice shelf model into one, similar to the situation depicted in Figure 1 (top). Although this model is still not capable of dynamically changing the boundary between all different systems, *Ritz et al.* [2001] dynamically change this boundary as a function of effective pressure.

[13] The difference between the ice sheet and shelf arises because the shelf is floating and because it experiences vanishing tangential traction on the bottom as well as the upper surface [*Hindmarsh*, 1993]. The length of the transition zone is then determined by the distance over which this vanishing traction occurs. For instance, a fast flowing ice stream owes its existence to a reduction in basal traction from values typical of ice sheet flow to negligible values over horizontal length scales much greater than the thickness of the ice sheet. Vanishing traction toward the grounding line is introduced through a friction parameter β^2 [*MacAyeal*, 1993], that relates the basal velocity to the basal drag (Figure 1, bottom). For $\beta^2 = 0$, basal drag equals zero (no traction) which is a situation similar to an ice shelf; for $\beta^2 = +\infty$, the basal velocity equals zero (ice frozen to the bedrock) which is valid for the ice sheet; for $0 < \beta^2 \ll +\infty$ a transition zone exists. We shall not consider the physical

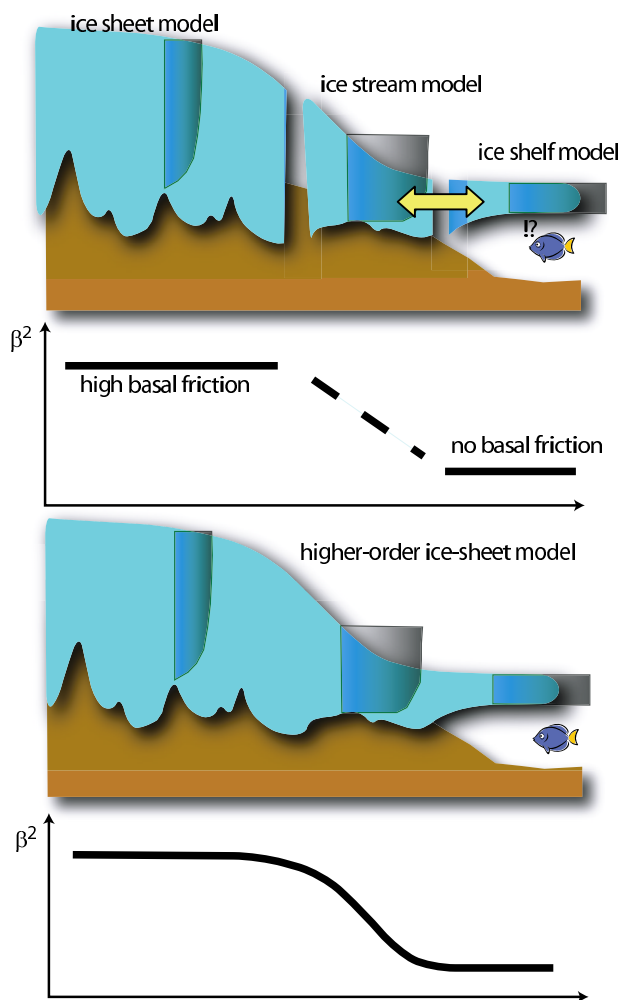


Figure 1. Sketch of the representation of stress transfer across the grounding line (top) in common ice sheet models and (bottom) in the higher-order model presented in this paper. The double arrow indicates where stress transmission between different models takes place.

mechanisms that are responsible for the reduction in traction (i.e., sliding) but suppose basal friction to be of the general form

$$\beta^2 = \exp[\beta_0(x_g - x)] \quad (9)$$

where β_0 (km^{-1}) controls the length of the transition zone (Figure 2). The exponential form of the basal friction relationship (9) stems from an analysis of the longitudinal profile of PIG (Figure 3). On the basis of the present-day geometry (surface and bedrock elevation profile), a control method has been applied to determine the basal friction coefficient β^2 along the transect of PIG from observed velocities, similar to the method presented by *Vieli and Payne* [2003] (B. De Smedt and F. Pattyn, manuscript in preparation, 2006). The smooth curve that runs through Figure 3 clearly depicts the exponential nature of the basal friction profile in the vicinity of the grounding line. Although the exponential form implies that at the grounding line $\beta^2 = 1.0$, where it should be zero by definition, this

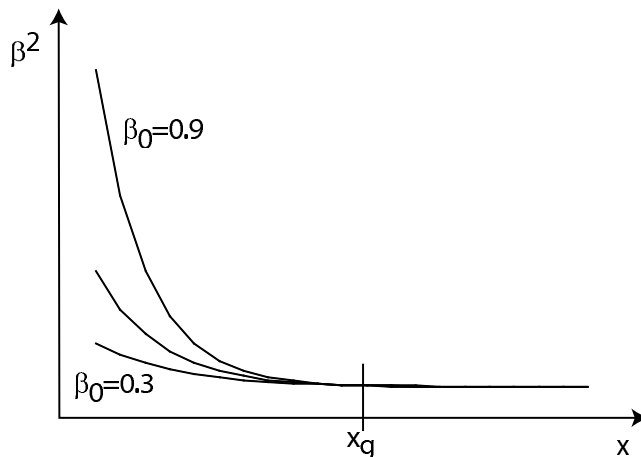


Figure 2. Basal friction β^2 near the grounding line x_g for different values of β_0 according to (9).

value is so small that it has no effect at all on the model results.

[14] β_0 can be interpreted as the inverse of a characteristic length scale $L = 1/\beta_0$. However, such a length scale is not representative for defining the length of the transition zone as β_0 is intrinsically influenced by effects of lateral drag and basal properties, that are not taken into account in this simple parameterization. Furthermore, this length scale does not coincide with the zone of influence in terms of longitudinal stress coupling between the ice sheet and the ice shelf and we therefore refrain from using L .

[15] Linking the subgrid determination of the position of the grounding line directly with the stress field within the ice sheet is a novel approach. There is no need to a priori prescribe what is ice sheet, ice stream or ice shelf and (9) is independent of the chosen grid size, which make the basal conditions independent of grid size as well. In addition, an advantage of (9) is that any singularity at the grounding line, defined by the abrupt transition between an ice sheet frozen to the bed ($\beta^2 = +\infty$) and a floating ice shelf ($\beta^2 = 0$), is

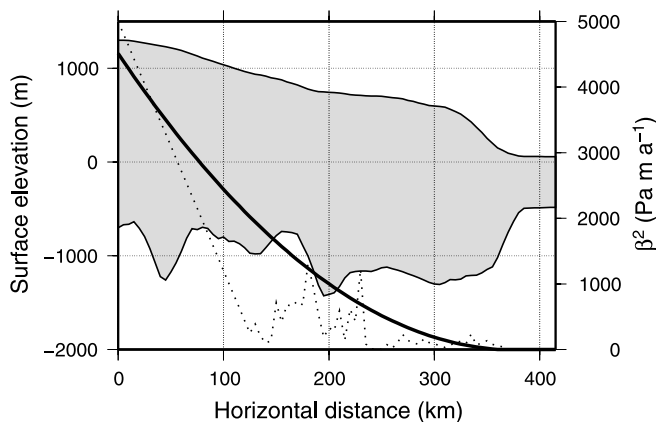


Figure 3. Longitudinal profile of the downstream portion of Pine Island Glacier (PIG), Antarctica, and the corresponding basal friction coefficient β^2 determined from a control method (dotted line). The exponential nature of the β^2 profile is given by the thick line. The grounding line is situated at $x = 380$ km.

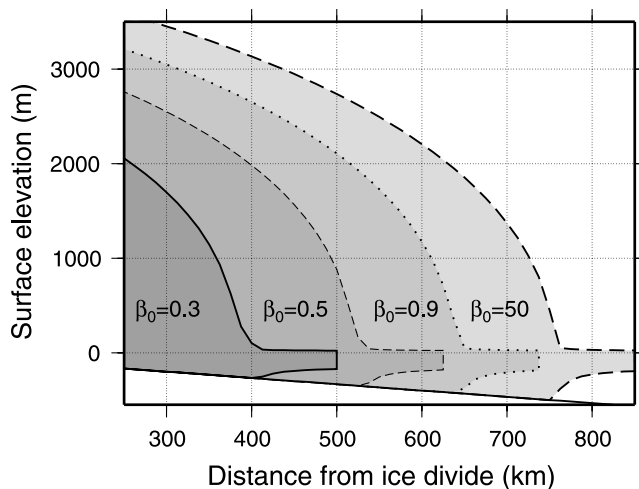


Figure 4. Equilibrium profiles of a marine ice sheet on a sloping bedrock for different sizes β_0 of the transition zone between the ice sheet and the ice shelf. All experiments started from a fixed grounding line at $x = 750$ km.

avoided. However, using (9) is equivalent to a transition zone of constant length in space and time. This could eventually lead to an unstable behavior for low values of β_0 .

[16] In reality, β^2 will be a function of basal characteristics, such as till strength or subglacial water flux or pressure [Pattyn et al., 2005]. Therefore a number of experiments were carried out in which a more realistic basal boundary condition was considered, i.e., by determining the basal friction pattern in the grounded ice sheet using a common sliding law as a function of the basal shear stress (in combination with (9) for the position of the grounding line itself). Apart from some differences related to sliding/no sliding conditions within the ice sheet, the qualitative behavior of these model experiments were similar to the experiments carried out in this paper using (9).

3. Sensitivity Experiments

[17] Following Vieli and Payne [2005], a typical WAIS model setup is considered, i.e., a flow line of 1000 km in length with a grid size of 12.5 km (81 grid points). The bed has a slope of -0.0006° . The surface mass balance (accumulation) was set to $\dot{a} = 0.2 \text{ m yr}^{-1}$. Initially, an ice sheet was formed with a grounding line fixed at 750 km from the ice divide, leaving an ice shelf of 250 km in length. Once the ice sheet reached a steady state, the grounding line was allowed to move freely and the model was run forward again to reach a new steady state (Figure 4).

3.1. Effect of Varying β_0

[18] The experiments were carried out for different values of β_0 , ranging from $\beta_0 = 50$ (transition zone of the order of one or a few ice thicknesses) to $\beta_0 = 0.3$. This leads to a retreat of the grounding line for $\beta_0 < 1.0$ before a new steady state is reached (Figure 4). The smallest ice sheet geometry is obtained for the smallest value of β_0 . For $\beta_0 = 50$, the grounding line remains positioned where it was initially fixed, i.e., at 750 km from the ice divide.

[19] The length of the transition zone in each of these experiments can eventually be derived from the profiles of

the driving stress τ_d along the flow line (Figure 5); for $\beta_0 = 0.3$ the ice sheet surface profile is concave upstream of the grounding line, typical for ice streams, and the maximum driving stress τ_d is reached 40 km upstream of the grounding line, compared to 10 km for $\beta_0 = 50$. Although lower values of β_0 were explored, the ice sheet configurations became too small to be useful. This is due to the fact that lateral drag was not taken into account at this stage.

[20] Using this information, qualitative rheomechanical properties for the structure of the sheet-stream-shelf transition can be assigned to the different values of β_0 , which are listed in Table 1. For instance $\beta_0 = 50$ corresponds to a sharp transition between the ice sheet and ice shelf, hence implying the lack of a transition zone, which is a quite common boundary around the East Antarctic coast [e.g., Mayer and Huybrechts, 1999]. In that case, longitudinal stresses are generally much smaller than shear stresses. Large outlet glaciers, such as Shirase Glacier, that drain the East Antarctic ice sheet are characterized by transition zones that are larger than one or a few ice thicknesses [Pattyn and Derauw, 2002]. Such transition zones are so-called meso-contraction stream zones [Hindmarsh, 1993], where longitudinal stresses are of the order of magnitude as shear stresses. Finally, small values of β_0 correspond to shelfy stream zones, such as the transition zone of PIG. Here, longitudinal stresses are dominant over shear stresses and longitudinal coupling becomes the most effective.

3.2. Neutral Equilibrium Hypothesis

[21] According to Hindmarsh [1993], an infinity of equilibrium profiles for a range of ice sheet grounding line positions and bed geometries exists, which implies neutral equilibrium of the grounding line. However, such a situation only applies to a marine ice sheet described by the shallow ice approximation that has no mechanical coupling to an ice shelf. Hindmarsh [1993] furthermore showed that such neutral equilibrium is an attractive state, meaning the system is stable and finds a steady state after a small perturbation. Ice streams, however, which broaden the transition zone, may have a stabilizing effect on the coupled system. The results of Vieli and Payne [2005] show that for any external forcing, the grounding line changes and finds a

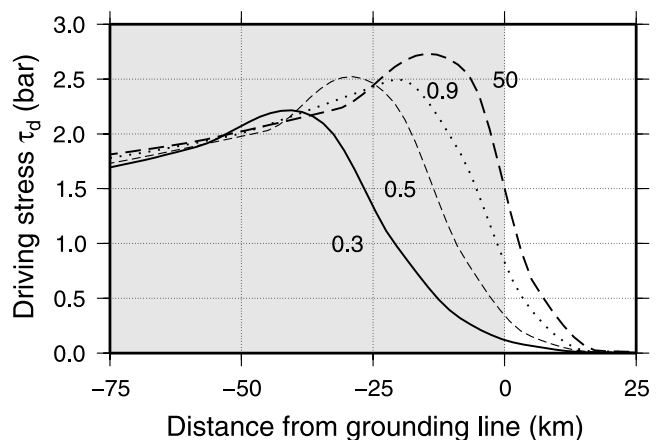


Figure 5. Driving stress profiles near the grounding line for the ice sheet experiments displayed in Figure 4. The grounded ice part is shaded.

Table 1. Qualitative Determination of the Width of the Transition Zone, Following *Hindmarsh* [1993]

Transition Zone	β_0 , km ⁻¹	Stress Type	Example
No/small transition zone	50	$\tau_{xx} \ll \tau_{xz}$	Ekströmsisen (East Antarctica) [<i>Mayer and Huybrechts</i> , 1999]
Mesotraction stream zone	0.5–1.0	$\tau_{xx} \sim \tau_{xz}$	Shirase Glacier (East Antarctica) [<i>Pattyn and Derauw</i> , 2002]
Shelfy stream zone	≤ 0.3	$\tau_{xx} \gg \tau_{xz}$	PIG (West Antarctica) [<i>Payne et al.</i> , 2004]

new steady state position, but the amount of change is in general small and no preference for an advance or retreat is observed. Furthermore, all experiments with moving grid models are reversible. The stable behavior is a characteristic dynamical features of a marine ice sheet with the property of neutral equilibrium.

[22] To investigate the equilibria of the ice sheet/shelf system, the four profiles shown in Figure 4 were perturbed with a mass balance perturbation of 1 m yr⁻¹ for a period of 5000 years, after which the mass balance was set back to 0.2 m yr⁻¹ until a new steady state of the ice sheet system was reached [*Vieli and Payne*, 2005]. In all cases this leads to a grounding line advance during the first 5000 year, increasing with decreasing values of β_0 (Figure 6). Grounding line advance depends on both the local water depth (geometry) and the ice flux; higher basal ice velocities (low values of β_0) increase the sensitivity for advancing. The limit for such advance depends on the balance between ice flux at the grounding line and the increase in surface mass accumulation, which makes that the advance for $\beta_0 = 0.3$ is smaller than the advance for $\beta_0 = 0.5$ (Figure 6).

[23] Grounding line retreat after the perturbation is clearly a function of transition zone characteristics. The retreat is minimal for small transition zones, i.e., $\beta_0 = 50$, and the grounding line remains more or less where it is. However, the reversibility of the process increases with the length of the transition zone. These results corroborate the neutral equilibrium hypothesis of *Hindmarsh* [1993], i.e., that for a small transition zone multiple equilibria may exist, therefore not necessarily exhibiting reversibility. For $\beta_0 \leq 1.0$ the grounding line returns to its initial position, which is a reversible process, similar to the behavior of moving grid models [*Vieli and Payne*, 2005]. Thus, according to our

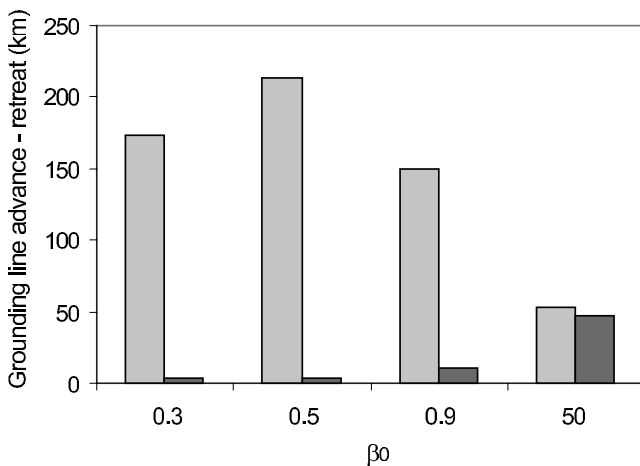


Figure 6. Relative grounding line position in response to a mass balance perturbation for different lengths of the transition zone (light shaded bars) and after the perturbation (dark shaded bars).

model results, grounding line migration for small transition zones exhibits hysteresis, while for larger transition zones the migration process is reversible. Therefore large transition zones facilitate grounding line migration in any direction. The amplitude of the grounding line migration is also a function of transition zone length.

3.3. Marine Ice Sheet Instability

[24] The situation is different when other types of bedrock are considered, such as a horizontal bed and a upsloping bed toward the coast. In both cases the ice sheet equilibrium is stable for a small transition zone ($\beta_0 = 50$), both in steady state and for a mass balance perturbation. When trying to obtain a steady state, an unstable ice sheet configuration results for $\beta_0 < 1.0$ on a horizontal bed (Figure 7). We believe that such a result is not unusual, as a number of physical processes are neglected in the model. First of all, the modeled ice sheet does not experience buttressing from the sides nor from the inland ice sheet. In reality, such a situation does not occur, as fast flow is always embedded in zones of slower flow. Three-dimensional experiments with a higher-order ice sheet model showed that fast ice flow (more than two orders of magnitude faster than the surrounding ice) can be stable on a flat bed [*Pattyn*, 2003]. Secondly, transition zone length is kept constant in space and time, irrespective of subglacial processes, that might eventually have a stabilizing effect on the ice flow.

4. Perturbations

4.1. Without Lateral Drag

[25] The sensitivity of transition zones is investigated through a number of perturbation experiments. Starting from the initial conditions (Figure 4), four perturbation experiments were carried out for a small transition zone, a mesotraction stream zone and a shelfy stream zone ($\beta_0 = 50$, 0.9 and 0.3, respectively). The perturbations include (A) basal melting at the grounding line of 1 m yr⁻¹, (B) bottom

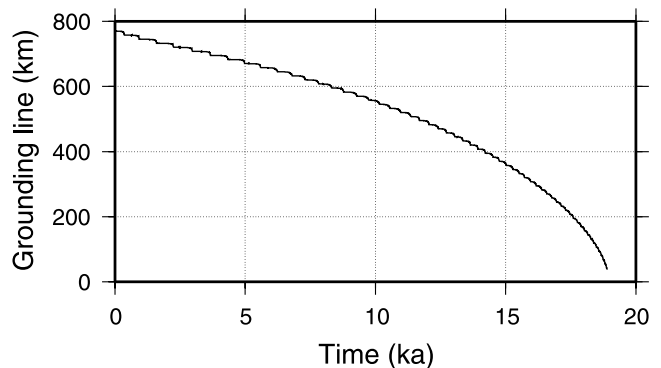


Figure 7. Accelerated retreat of the grounding line for an ice sheet resting on a flat bedrock and a transition zone length determined by $\beta_0 = 0.9$.

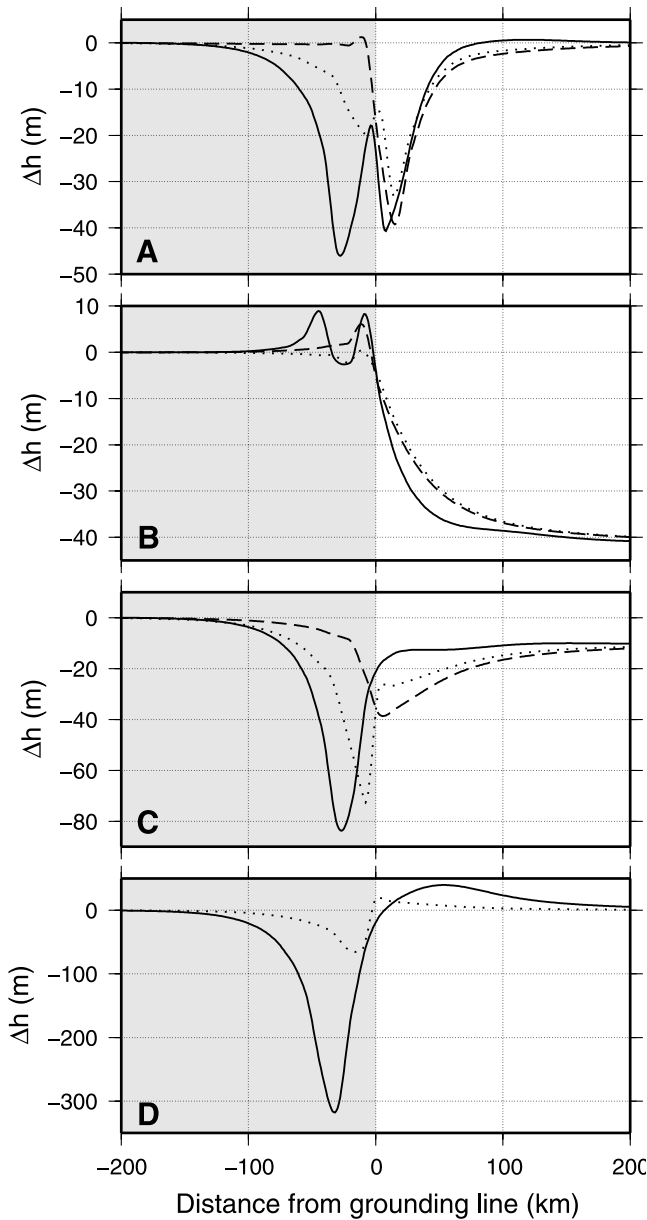


Figure 8. Ice sheet response near the grounding line to different perturbation for $\beta_0 = 50$ (dashed line), 0.9 (dotted line) and 0.3 (solid line) after 100 year. (a) Melting of 1 m yr^{-1} at the grounding line. (b) Melting of 0.5 m yr^{-1} along the whole length of the ice shelf. (c) Reduced ice shelf buttressing (see text for details). (d) Decrease in β_0 , from $\beta_0 = 0.9$ to 0.7 and from $\beta_0 = 0.3$ to 0.2 . The grounded ice part is shaded.

melting below the ice shelf of 0.5 m yr^{-1} , (C) a 20% increase of σ_e in (2), which is equivalent to reduced buttressing, and (D) a decrease in β_0 , which is equivalent to enlarging the transition zone. The impact of these perturbations on the ice sheet system after 100 year is displayed in Figure 8.

[26] All perturbations affect in one way or another the ice thickness within the ice sheet and/or shelf. For a small transition zone ($\beta_0 = 50$), there is no inland transmission of any of the perturbations. Large transition zones allow for the

perturbation to be transmitted inland over large distances, larger than the extent of the stream zone as defined by the profiles of driving stress. For $\beta_0 = 0.3$ the perturbation is propagated inland over more than 100 km, even though the stream area, as defined by the profile of the driving stress in Figure 5, is limited to a zone of 30 km. This transmission results in immediate thinning of the inland ice sheet in most of the experiments.

[27] As explained by Payne *et al.* [2004], stress transfer across the grounding line leads to accelerated ice flow inland and thinning directly upstream, which can then diffuse rapidly inland. This was demonstrated by a decrease of β^2 at the grounding line [Payne *et al.*, 2004], resulting in a substantial inland thinning that reaches more than 100 km inland, as well as a thickening wave in the ice shelf, due to the accelerated ice transfer across the grounding line caused by higher ice speed. This behavior is confirmed by our experiment D, in which reduction of friction β^2 at the grounding line is simulated by widening the transition zone. However, the origin of the perturbation is inland (and not in the ocean) and results in a thickening of the floating part due to a higher ice flux across the grounding line.

[28] Observed thinning of PIG's ice shelf and the inland glacier was attributed to an increase of melting under the ice shelf due to higher ocean temperatures [Shepherd *et al.*, 2004]. However, according to experiment B, thinning of the ice shelf due to bottom melting seems to have no impact on the inland ice sheet, even in a case where stress transmission is favored (Figure 8b). Ice shelf thinning reduces creep rates in the (freely floating) ice shelf and slows down the shelf locally. In order to influence the inland ice sheet, either melting at or a decrease in friction upstream of the grounding line is necessary (Figures 8a and 8d).

[29] The only "real" marine perturbation that has a significant influence of the inland ice sheet is a reduction in buttressing, simulated here by increasing the creep rate at the ice shelf edge (Figure 8c). Also here, the inland propagation of the thinning wave is a function of the length of the transition zone, which corroborates the results by Dupont and Alley [2005], who investigated the transition between an ice stream (shelvy stream zone) and an ice shelf.

[30] In other words, if the origin of the thinning is inland (upstream from the grounding line), the ice sheet thins and the ice shelf thickens, due to the increased ice flux. If the thinning is marine in origin (due to decrease in buttressing or melting at the grounding line), an upstream propagation of the thinning signal will occur only when a sufficient large transition zone exists. However, melting under the ice shelf thins the shelf and has a stabilizing effect on the inland ice sheet irrespective the transition zone characteristics, since reduced creep rates slow down the ice flow near the grounding line.

4.2. Effects of Lateral Drag

[31] The results presented so far might eventually be biased by the omission of lateral drag along the ice sheet profile. Following the analysis of Van der Veen and Whillans [1996], lateral resistance can be parameterized in terms of ice stream width W and velocity u given by

$$\tau_L = -\frac{h}{W} \left(\frac{5u}{2AW} \right)^{1/3} \quad (10)$$

Considering a constant width W along the ice sheet profile, (10) can be rewritten as $\tau_L = \gamma hu$. Since near the grounding line $u \approx u_b$, the basal boundary condition (3) becomes

$$4\eta \frac{\partial u_b}{\partial x} \frac{\partial z_b}{\partial x} - 2\eta \frac{\partial u_b}{\partial z} - u_b(\beta^2 + \gamma h) = 0 \quad (11)$$

Therefore, by omitting the lateral resistance we implicitly include a linearized version (constant W) of this parameterization subsumed within the resistance of the bed [Vieli and Payne, 2005]. The effect of lateral resistance on the perturbations should therefore be minimal as it can be translated into a different value of β_0 . To test this, we included lateral drag as parameterized in (11) in experiment B. Values for γ were chosen in such a way that inclusion of lateral drag according to (11) resulted in a forward grounding line movement over several grid points (30 to 100 km) starting from the standard experiment with $\beta_0 = 0.3$. The model was run forward until a new steady state ice sheet profile was reached. Each of these profiles were then perturbed with a melting rate of 0.5 m yr^{-1} along the whole ice shelf, similar to experiment B. The results shown in Figure 9 underscore the stabilizing effect of increasing lateral drag, i.e., that even with lateral drag there is no thinning propagation upstream of the grounding line. On the contrary, later drag makes the ice sheet thickening upstream from the grounding line. However, according to (11), thinning of the ice shelf reduces its thickness h , and hence reduces the lateral drag $\tau_L = \gamma uh$. Our experiment thus clearly demonstrates that the reduced creep rates due to melting are more important than the associated thinning.

5. Conclusions

[32] On the basis of a higher-order ice sheet model [Patyn, 2002], dynamic grounding line migration was implemented with subgrid accuracy, so that the time-dependent behavior of marine ice sheets could be investigated. The model is capable of simulating the dynamic migration of the grounding line, thereby taking into account longitudinal stress coupling across the transition zone.

[33] Sensitivity experiments demonstrate that grounding line migration for small transition zones exhibits hysteresis, while for larger transition zones, such as mesotraction stream zones and shelfy stream zones, the migration process is reversible. Therefore large transition zones facilitate grounding line migration in any direction. Furthermore, the amplitude of the grounding line migration is also a function of transition zone length.

[34] From the perturbation experiments it is clear that as long as the transition zone between ice sheet and shelf is narrow there is no upstream stress transfer due to perturbations in the ice shelf and at the grounding line, nor any acceleration of the inland ice flow. Such a situation has been observed in the field [Mayer and Huybrechts, 1999] and is also corroborated by model experiments [Lestringant, 1994]. However, most of the discharge of the Antarctic ice sheet is through large outlet glaciers or ice streams with transition zones of the mesotraction stream type. Even though mesotraction stream zones are much smaller than shelfy stream zones and thought to be passive transition zones, stress

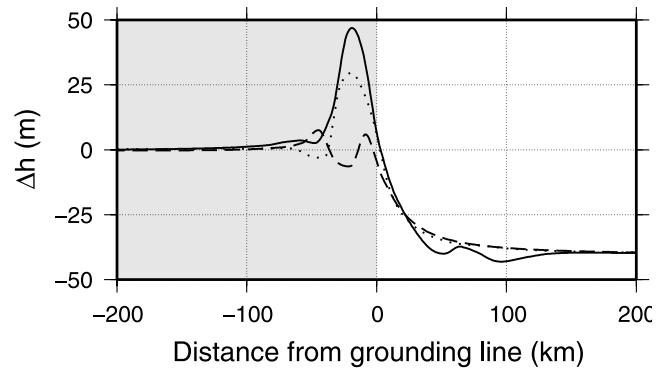


Figure 9. Ice sheet response near the grounding line to melting of 0.5 m yr^{-1} along the whole length of the ice shelf for $\gamma = 0$ (dashed line), 0.60 (dotted line), and 0.65 (solid line). Results are shown after 100 years for the ice stream case $\beta_0 = 0.3$. The grounded ice part is shaded.

transmission across the grounding line is still favored in such a case and perturbations at the grounding line can result in a significant inland thinning. This would make them more sensitive to change than previously thought of.

[35] Sensitivity of the ice sheet system increases with increasing length of the transition zone and allows for a rapid propagation of inland thinning. Hence accelerated inland thinning and grounding line retreat of shelfy streams (such as PIG), are either due to a reduction in ice shelf buttressing or due to perturbations at or upstream of the grounding line. Reduced traction or increased basal melting are examples of such perturbations. Ice shelf bottom melting slows down the ice shelf flow and has no influence on the dynamics of the inland ice sheet, irrespective of the length of the transition zone, except if this thinning is associated with a change in buttressing effect. Including lateral drag in the model does not alter the results qualitatively.

[36] Our model experiments show that as long as transition zones are small, ice shelves have no influence on the inland ice sheet. For larger transition zones (mesotraction stream zone and shelfy stream zone) ice shelves do matter and the balance of forces in the transition zone needs to take care of both vertical shear and longitudinal stress gradients.

Appendix A: Numerical Treatment

[37] A common procedure in solving finite difference ice sheet models is to rewrite the ice thickness equation (4) as a diffusion equation for ice thickness h , i.e.,

$$\frac{\partial h}{\partial t} - \frac{\partial}{\partial x} \left(D \frac{\partial h}{\partial x} \right) = \frac{\partial}{\partial x} \left(D \frac{\partial b}{\partial x} \right) + \dot{a} - \dot{m}, \quad (A1)$$

where $D = q (\partial s / \partial x)^{-1}$. This results in a tridiagonal system of equations, and is solved using the tridiagonal algorithm of Press et al. [1992]. For the ice shelf (floating part), diffusivities do not work and the flux divergence equation (4) is kept. At the grounding line node (defined as the last grounded grid point) upstream fluxes are determined using diffusivities, while downstream fluxes are based on q [Huybrechts, 1992]. Such a scheme has the

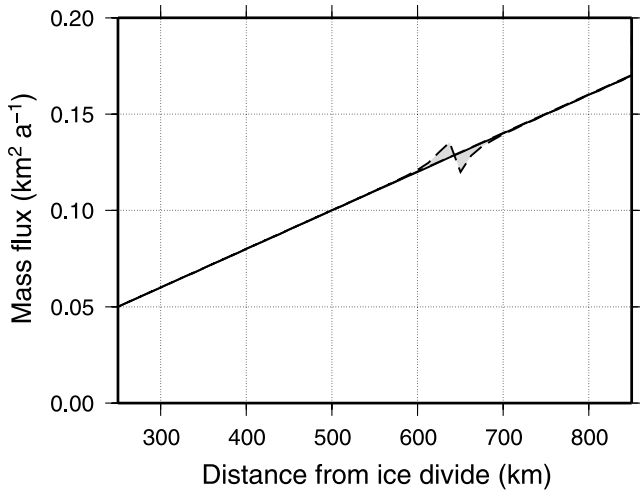


Figure A1. Steady state mass flux q along the flow line according to the transport equation (A2) (solid line) and by combining diffusivities for the ice sheet and fluxes for the ice shelf (dotted line) for the experiment with $\beta_0 = 0.9$. In steady state and for a constant surface mass balance (no melting) along the flow line, mass flux must obey a straight line defined by $q = \dot{a} \cdot x$. Note the small inconsistency near the grounding line for the combined scheme.

advantage of being numerically stable, but is not completely mass conservative across the grounding line (Figure A1).

[38] To overcome the mass conservation problem across the grounding line a solution is obtained using a transport equation. To stabilize the equation a small artificial diffusion term is added and the convective term is written as a linear combination between a central and an upwind biased difference [Polanco and May, 2000]. The finite difference approximation is written as

$$\frac{h_j^{(n+1)} - h_j^{(n)}}{\Delta t} = \dot{a} - \dot{m} + \mathcal{D} \left(\frac{h_{j+1}^{(n)} - 2h_j^{(n)} + h_{j-1}^{(n)}}{(\Delta x)^2} \right) - (1 - \omega) \left(\frac{q_{j+1}^{(n)} - q_{j-1}^{(n)}}{2\Delta x} \right) - \omega \left(\frac{3q_j^{(n)} - 4q_{j-1}^{(n)} + q_{j-2}^{(n)}}{2\Delta x} \right), \quad (\text{A2})$$

where $\omega = 0.5$ and \mathcal{D} is an artificial diffusion term, taken in such a way that the equation becomes stable without influencing the result quantitatively. A trade-off was found with a value of $\mathcal{D} = 10^4$. Using this solution scheme, mass is conserved across the grounding line (Figure A1). However, the scheme is less stable than the combined one based on (A1) and small time steps need to be chosen. Furthermore, comparison between the numerical result of both schemes did not reveal a different behavior, so that for most of the experiments presented here the more stable scheme was preferred.

[39] **Acknowledgments.** This paper forms a contribution to the Belgian Research Programme on the Antarctic (Belgian Federal Science Policy Office). A.H. and B.D.S. are supported by the Fund for Scientific Research, Flanders (FWO-Vlaanderen); S.D.B. is supported by the Institute for the Promotion of Innovation by Science and Technology in Flanders (IWT-Vlaanderen).

References

- Bentley, C. (1998), Ice on the fast track, *Nature*, *394*, 21–22.
- Dupont, T., and R. Alley (2005), Assessment of the importance of ice-shelf buttressing to ice-sheet flow, *Geophys. Res. Lett.*, *32*, L04503, doi:10.1029/2004GL022024.
- Herterich, K. (1987), On the flow within the transition zone between ice sheet and ice shelf, in *Dynamics of the West Antarctic Ice Sheet*, edited by C. Van der Veen, and J. Oerlemans, pp. 185–202, Springer, New York.
- Hindmarsh, R. (1993), Qualitative dynamics of marine ice sheets, in *Ice in the Climate System, NATO ASI Ser., Ser. I*, vol. 12, edited by W. Peltier, pp. 67–99, Springer, New York.
- Hindmarsh, R. (1996), Stability of ice rises and uncoupled marine ice sheets, *Ann. Glaciol.*, *23*, 105–115.
- Hindmarsh, R., and E. Le Meur (2001), Dynamical processes involved in the retreat of marine ice sheets, *J. Glaciol.*, *47*(157), 271–282.
- Hulbe, C., and D. MacAyeal (1999), A new numerical model of coupled inland ice sheet, ice stream, and ice shelf flow and its application to the West Antarctic ice sheet, *J. Geophys. Res.*, *104*(B11), 25,349–25,366.
- Hutter, K. (1983), *Theoretical Glaciology*, Springer, New York.
- Huybrechts, P. (1992), The Antarctic ice sheet and environmental change: A three-dimensional modelling study, *Ber. Polarforsch.*, *99*, 1–241.
- Huybrechts, P., A. Abe-Ouchi, I. Marsiat, F. Pattyn, T. Payne, C. Ritz, and V. Rommelaere (1998), Report of the Third EISMINT Workshop on Model Intercomparison, 140 pp., Eur. Sci. Found., Strasbourg, France.
- Lestringant, R. (1994), A two-dimensional finite-element study of flow in the transition zone between an ice sheet and an ice shelf, *Ann. Glaciol.*, *20*, 67–72.
- MacAyeal, D. (1993), A tutorial on the use of control methods in ice-sheet modeling, *J. Glaciol.*, *39*(131), 91–98.
- Mayer, C., and P. Huybrechts (1999), Ice-dynamic conditions across the grounding zone, Ekströmisen, East Antarctica, *J. Glaciol.*, *45*(150), 384–393.
- Paterson, W. (1994), *The Physics of Glaciers*, 3rd ed., Elsevier, New York.
- Pattyn, F. (2002), Transient glacier response with a higher-order numerical ice-flow model, *J. Glaciol.*, *48*(162), 467–477.
- Pattyn, F. (2003), A new three-dimensional higher-order thermomechanical ice sheet model: Basic sensitivity, ice stream development, and ice flow across subglacial lakes, *J. Geophys. Res.*, *108*(B8), 2382, doi:10.1029/2002JB002329.
- Pattyn, F., and D. Derauw (2002), Ice-dynamic conditions of Shirase Glacier, Antarctica, inferred from ERS-SAR interferometry, *J. Glaciol.*, *48*(163), 559–565.
- Pattyn, F., S. De Brabander, and A. Huyghe (2005), Basal and thermal control mechanisms of the Ragnhild glaciers, East Antarctica, *Ann. Glaciol.*, *40*, 225–231.
- Payne, A., A. Vieli, A. Shepherd, D. Wingham, and E. Rignot (2004), Recent dramatic thinning of largest West Antarctic ice stream triggered by oceans, *Geophys. Res. Lett.*, *31*, L23401, doi:10.1029/2004GL021284.
- Polanco, F., and R. May (2000), An implicit finite difference approximation to the one-dimensional transport equation, *ANZIAM J.*, *42*(E), C1179–C1198.
- Press, W., S. Teukolsky, W. Vetterling, and B. Flannery (1992), *Numerical Recipes in C: The Art of Scientific Computing*, 2nd ed., 994 pp., Cambridge Univ. Press, New York.
- Rignot, E. (1998), Fast recession of a West Antarctic glacier, *Science*, *281*(5376), 549–551.
- Rignot, E., G. Casassa, P. Gogineni, W. Krabill, A. Rivera, and R. Thomas (2004), Accelerated ice discharge from the Antarctic Peninsula following the collapse of Larsen B ice shelf, *Geophys. Res. Lett.*, *31*, L18401, doi:10.1029/2004GL020697.
- Ritz, C., V. Rommelaere, and C. Dumas (2001), Modeling the evolution of the Antarctic ice sheet over the last 420,000 years: Implications for altitude changes in the Vostok region, *J. Geophys. Res.*, *106*(D23), 31,943–31,964.
- Scambos, T., J. Bohlander, C. Shuman, and P. Skvarca (2004), Glacier acceleration and thinning after ice shelf collapse in the Larsen B embayment, *Geophys. Res. Lett.*, *31*, L18402, doi:10.1029/2004GL020670.
- Shepherd, A., D. Wingham, and E. Rignot (2004), Warm ocean is eroding West Antarctic Ice Sheet, *Geophys. Res. Lett.*, *31*, L23402, doi:10.1029/2004GL021106.
- Thomas, R. (1973), The creep of ice shelves: Theory, *J. Glaciol.*, *12*(64), 45–53.
- Thomas, R., and C. Bentley (1978), A model for Holocene retreat of the West Antarctic Ice Sheet, *Quat. Res.*, *10*, 150–170.
- Van der Veen, C. (1985), Response of a marine ice sheet to changes at the grounding line, *Quat. Res.*, *24*, 257–267.
- Van der Veen, C. (1999), *Fundamentals of Glacier Dynamics*, A. A. Balkema, Brookfield, Vt.

- Van der Veen, C., and I. Whillans (1996), Model experiments on the evolution and stability of ice streams, *Ann. Glaciol.*, 23, 129–137.
- Vieli, A., and A. Payne (2003), Application of control methods for modeling the flow of Pine Island Glacier, West Antarctica, *Ann. Glaciol.*, 36, 197–204.
- Vieli, A., and A. Payne (2005), Assessing the ability of numerical ice sheet models to simulate grounding line migration, *J. Geophys. Res.*, 110, F01003, doi:10.1029/2004JF000202.
- Whillans, I., and C. Van der Veen (1993), Patterns of calculated basal drag on Ice Streams B and C, Antarctica, *J. Glaciol.*, 39(133), 437–446.
- Wingham, D., A. Ridout, R. Scharroo, R. Arthern, and C. Shum (1998), Antarctic elevation change from 1992 to 1996, *Science*, 282, 456–458.
-
- S. De Brabander, B. De Smedt, and A. Huyghe, Department of Geography, Vrije Universiteit Brussel, Pleinlaan 2, B-1050 Bruxelles, Belgium.
- F. Pattyn, Laboratoire de Glaciologie, Département des Sciences de la Terre et de l'Environnement, Université Libre de Bruxelles, CP 160/03, Avenue F.D. Roosevelt, 50, B-1050 Bruxelles, Belgium. (fpattyn@ulb.ac.be)